

## Environmentally friendly antifouling transparent coatings based on sol-gel “epoxy/titanium tetrabutoxide” composition modified with detonation nanodiamond

© Olga A. Shilova<sup>a,b</sup> ✉, Irina B. Glebova<sup>a</sup>, Vadim I. Voshchikov<sup>a</sup>, Valery L. Ugolkov<sup>a</sup>, Valery Yu. Dolmatov<sup>c</sup>, Kseniya A. Komarova<sup>d</sup>, Alexandra G. Ivanova<sup>a</sup>

<sup>a</sup> Institute of Silicate Chemistry of Russian Academy of Sciences,  
2, Makarova Emb., Saint-Petersburg, 199034, Russian Federation,

<sup>b</sup> Saint-Petersburg State Electrotechnical University “LETI”,  
5, Prof. Popova St., Saint-Petersburg, 197022, Russian Federation,

<sup>c</sup> Special Design and Technology Bureau “Technolog”, 33-a, Sovetskii Pr., Saint-Petersburg, 192076, Russian Federation,

<sup>d</sup> A.N. Severtsov Institute of Ecology and Evolution of the Russian Academy of Sciences,  
33, Leninsky Pr., Moscow, 119071, Russian Federation

✉ olgashilova@bk.ru

**Abstract:** Transparent organic-inorganic coatings for the protection of optical glass were prepared by sol-gel processing using hydrogenated epoxy resin and titanium tetrabutoxide as precursors. Detonation nanodiamond (DND) was introduced into the sol-gel composition *in situ* to improve physic-mechanical and antifouling coatings properties. The processes of film-forming sols synthesis and organic-inorganic coatings formation, as well as the influence of DND on the processes of structure formation of these sols and the physic-mechanical properties of the obtained coatings, have been studied using IR-Fourier spectroscopy, thermal analysis combined with mass spectroscopy, and standard methods for studying paint coatings. The antifouling properties of the coatings on the magnifying glasses were tested in natural conditions, in the marine environment, at the climatic station of the Joint Russian-Vietnam Tropical Research and Test Center (Tropical Center, Nha Trang, SR Vietnam).

**Keywords:** sol-gel processing; detonation nanodiamond; organic-inorganic coatings; glass protection coatings; marine full-scale test.

**For citation:** Shilova OA, Glebova IB, Voshchikov VI, Ugolkov VL, Dolmatov VYu, Komarova KA, Ivanova AG. Environmentally friendly antifouling transparent coatings based on sol-gel ‘epoxy/titanium tetrabutoxide’ composition modified with detonation nanodiamond. *Journal of Advanced Materials and Technologies*. 2022;7(3):201-218. DOI: 10.17277/jamt.2022.03.pp.201-218

## Экологически безопасные прозрачные противообрастающие покрытия на основе золь-гель композиции «эпоксидная смола/тетрабутоксид титана», модифицированной детонационным наноалмазом

© О. А. Шилова<sup>a,b</sup> ✉, И. Б. Глебова<sup>a</sup>, В. И. Вошиков<sup>a</sup>, В. Л. Уголков<sup>a</sup>, В. Ю. Долматов<sup>c</sup>, К. А. Комарова<sup>d</sup>, А. Г. Иванова<sup>a</sup>

<sup>a</sup> Институт химии силикатов им. И.В. Гребенникова Российской академии наук,  
наб. Макарова, 2, Санкт-Петербург, 199034, Российская Федерация,

<sup>b</sup> Санкт-Петербургский государственный электротехнический университет «ЛЭТИ»,  
ул. Проф. Попова, 5, Санкт-Петербург, 199034, Российская Федерация,

<sup>c</sup> СКТБ «Техноло», 33-а, Советский пр., Санкт-Петербург, 192076, Российская Федерация,

<sup>d</sup> Институт проблем экологии и эволюции им. А.Н. Северцова Российской академии наук,  
Ленинский пр., 33, Москва, 119071, Российская Федерация

✉ olgashilova@bk.ru

**Аннотация:** Прозрачные органо-неорганические покрытия для защиты оптического стекла получены по золь-гель технологии на основе гидрированной эпоксидной смолы и тетрабутоксид титана. Для улучшения их физико-механических и противообрастающих свойств в золь-гель композиции в процессе их синтеза *in situ* введен

детонационный наноалмаз (ДНА) при варьировании его концентрации. С использованием ИК-Фурье спектроскопии, термического анализа, совмещенного с масс-спектрометрией, и стандартных методов изучения лакокрасочных покрытий исследованы процессы формирования пленкообразующих золь и органо-неорганических покрытий, а также влияние ДНА на процессы структурообразования золь и физико-механические свойства покрытий. Противообрастающие свойства разработанных покрытий, нанесенных на увеличительные стекла, испытаны в натурных условиях, морской среде, на климатической станции Совместного Российско-Вьетнамского Тропического научно-исследовательского и технологического центра (Тропический Центр, г. Нячанг, СР Вьетнам).

**Ключевые слова:** золь-гель процессы; органо-неорганические покрытия; детонационный наноалмаз; покрытия для защиты стекла; морские натурные испытания.

**Для цитирования:** Shilova OA, Glebova IB, Voshchikov VI, Ugolkov VL, Dolmatov VYu, Komarova KA, Ivanova AG. Environmentally friendly antifouling transparent coatings based on sol-gel 'epoxy/titanium tetrabutoxide' composition modified with detonation nanodiamond. *Journal of Advanced Materials and Technologies*. 2022;7(3):201-218. DOI: 10.17277/jamt.2022.03.pp.201-218

## 1. Introduction

Sol-gel technology is successfully used to produce transparent protective coatings for various purposes. This method is often used to prepare coatings based on  $\text{SiO}_2$  and  $\text{TiO}_2$ , using silicon and titanium alkoxides (tetraethoxysilane, titanium tetrabutoxide, or titanium isopropoxide) as precursors [1–5]. If high-temperature heat treatment of coatings is not allowed to fix them on substrates and give them the necessary physical and mechanical properties, organic-inorganic coatings are synthesized, which can be formed using cold curing. Epoxy resins and their adducts with alkoxy compounds, such as 3-glycidoxypropyltrimethoxysilane, 3-glycidoxypropyltriethoxysilane, (3-glycidoxypropyl) methyl-diethoxysilane, etc., are used as organic components [6–10]. The latter, due to the presence of ethoxy groups, promote the formation of covalent bonds between the epoxy and organosilicon structural networks. This is especially important because composites obtained on the basis of epoxy resins and tetraethoxysilane hydrolysis products are prone to phase separation [11]. To avoid phase separation,

instead of epoxy resins, their hydrogenated analogs can be used, as we did earlier when using EPONEX 1510 resin as a hydrogenated analog of ED-20 resin (Fig. 1) [12, 13].

Often, organosilicon compounds are added to sol-gel compositions, including those based on epoxy resin and silicon and titanium alkoxides, which also improves the adhesion and physico-mechanical properties of the resulting coatings [7, 10].

Curing agents of various types are introduced into organic-inorganic sol-gel compositions based on epoxy resin, including those containing silicon and titanium alkoxides [6–10, 14]. Conventionally, they can be divided into two large groups. First of all, these are compounds that contribute to the chemical interaction of the curing agent with the epoxy oligomer due to the presence of active functional groups (amines, aldehydes). They also include catalysts, under the action of which the polymerization reaction is carried out with the opening of the epoxy ring and the formation of a three-dimensional network structure. Most often, various amines are used, which provide a fairly fast curing of epoxides and do not

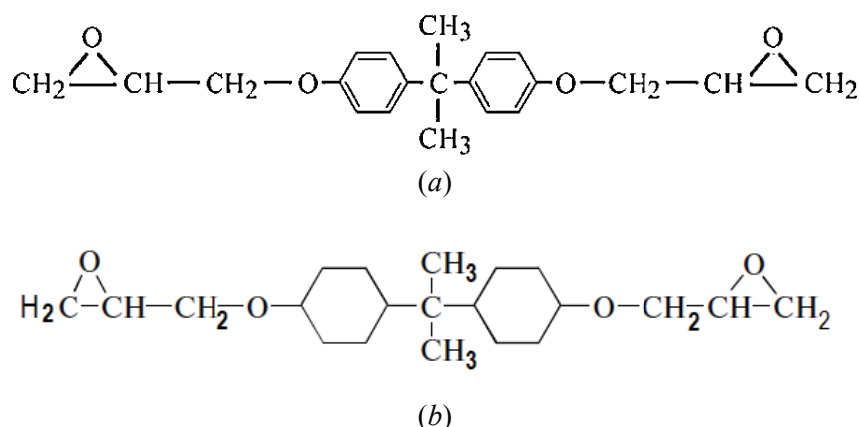


**Fig. 1.** Structural formulas of commercial epoxy resin ED-20 (a) and its hydrogenated analog – resin EPONEX 1510 (b)

require high-temperature processing. There are many examples in the literature of the use of  $\gamma$ -aminopropyltriethoxysilane (AGM-9), which, on the one hand, acts as an amine hardener, and, on the other hand, provides crosslinking with alkoxy compounds, thus preventing phase separation [15, 16]. Catalytic curing of epoxy oligomers is less commonly used. As such catalysts, Lewis acids (in particular, boron trifluoride) can be used, which are most promising for obtaining sol-gel film-forming compositions, since gelation processes in them occur more slowly than when using amine hardeners [12, 13, 17].

Small amounts of fillers are introduced into the coatings to improve the properties of coatings produced by the sol-gel technology, i.e. to improve the physical and mechanical properties, increase temperature stability, impart biostability, optical and other special properties. The most popular nanoparticles are  $\text{SiO}_2$ ,  $\text{TiO}_2$  [14–16, 18, 19], as well as carbon nanoparticles, including ultradispersed diamond (in the concentration range of 0.25–0.75 mass parts) [14] and detonation nanodiamond (DND) [12, 13, 17, 20].

DND nanoparticles are characterized by an isotropic structure and properties due to both the high symmetry of the cubic lattice of a nanodiamond single crystal and the random nature of aggregation of primary particles [21]. This distinguishes DND nanoparticles from different types of carbon fibers with their linear anisotropy, as well as from carbon black and fillers with a graphite structure, which have a pronounced layered structure. Therefore, it can be assumed that DND as a filler should promote the formation of more perfect three-dimensional structures of polymer composites. One should expect the improvement in the whole range of physico-mechanical properties of polymer-nanodiamond composites, including strength, wear resistance, thermal and chemical stability, etc. Quite a lot of work has been devoted to studying the efficiency of introducing DND into elastomer and polymer matrices to improve their elastic strength and tribotechnical characteristics [22–25]. However, there

are not so many works devoted to studying the processes occurring in sol-gel composites in the presence of diamond nanoparticles. The authors of [26] found a decrease in the defectiveness of the coating structure upon the introduction of hydroxylated nanodiamond into sols in amounts of 0.005, 0.01, 0.02, and 0.05 wt. %. Our studies of the mesostructure of composites based on tetraethoxysilane and DND-modified epoxy resins have shown that DND acts as a structure-forming agent [12, 13, 27].

Studies of the DND effect on the structure of organic-inorganic coatings produced from sol-gel compositions based on epoxy resins and titanium alkoxides are even scarcer. In the monograph [28], we presented the results of studying the fungicidal activity and supramolecular (mesostructure) of coatings produced from sols based on titanium alkoxides, including with additives of photocatalytically active  $\text{TiO}_2$  nanoparticles.

The aim of this paper is to study the physicochemical processes of structure formation in multicomponent organic-inorganic sols based on epoxy resin and titanium alkoxide as they mature and form films, including in the presence of DND nanoparticles, as well as to study the effect of DND on the thermal evolution of the composition of coatings and on their physico-mechanical and antifouling properties.

## 2. Materials and Methods

### 2.1. Synthesis of sol-gel compositions and preparation of coatings

Tetrabutoxytitanium (TBT)  $\text{Ti}(\text{OBU})_4$  was used as a precursor to obtain a film-forming sol, to which acetylacetone (AcAc), ethyl cellosolve, and 1 N aqueous solution of nitric acid were sequentially added with vigorous stirring to initiate the acid hydrolysis of TBT (Fig. 2). Component ratio (wt. %): TBT, 21.3; AcAc, 6.3; ethyl cellosolve, 42.1;  $\text{HNO}_3$ , 7.2; Eponex 1510 – 21.3,  $\text{BF}_3$  – 2.8.

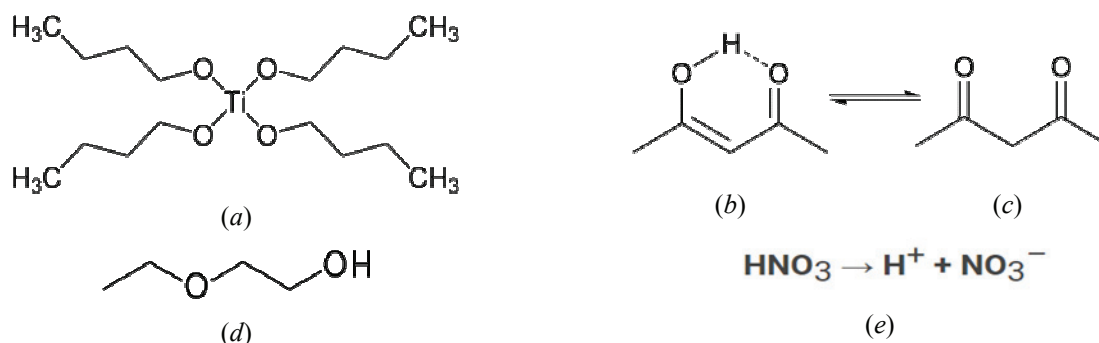


**Fig. 2.** Structural formulas of the initial components of the epoxy-titanate sol:

tetrabutoxytitanium (a), acetylacetone: enol (b) and ketone (c) forms, ethyl cellosolve (d), 1 N aqueous  $\text{HNO}_3$  solution (e)

The choice of AcAc as a solvent is due to the fact that it forms strong complexes with TBT, which reduce the rate of TBT hydrolysis and its completeness [29]. This contributes to the sedimentation and aggregation stability of the sol, which remains in the stage of active film formation for a longer time. Ethyl cellosolve is known as a solvent that is miscible with almost all known solvents at room temperature and at the same time it dissolves in water. Thus, it contributes to the uniformity of the structure of the resulting sols and coatings based on them.

Next, EPONEX 1510 epoxy resin (epoxy number = 20.04 %,  $\rho = 1.14 \text{ g}\cdot\text{cm}^{-3}$ ) was added to the resulting mixture (see Fig. 1) at a mass ratio of TBT/EPONEX 1510 = 21/21. The catalyst used was a solution of boron trifluoride in diethylene glycol (2 wt. %  $\text{BF}_3$  with respect to the epoxy resin), which caused the ionic polymerization reaction of the epoxy resin to proceed according to the cationic type. Before further use, the resulting mixtures were kept in a closed container in air for at least 1 hour. Sols, which were additionally processed in a vacuum cabinet for 2 hours and heated to 80 °C, were also chosen for the study. The gelation process occurred both at room temperature and at a temperature of 120 °C for 2 hours.

As a biocidal additive, DND (SKTB “Technolog”, St. Petersburg, Russia) was introduced into the prepared sols in the form of an aqueous suspension – 0.2 or 0.4 wt. % DND.

The coatings on the protected surfaces were applied by airbrush or by pouring. To study the properties of coatings, glass slides 75×25×2 mm in size were used as substrates (to determine the contact angle and hardness of coatings) and plates made of steel grade PS 08 150×70×1 mm in size (to determine the adhesion of coatings). For full-scale tests at sea, coatings were applied to hand-held magnifying glasses (loupes) with a diameter of 100 mm.

## 2.2. Methodology of laboratory tests

The following physico-mechanical properties of the coatings were investigated: contact angle, hardness and adhesion.

The contact angle characterizes the hydrophobicity of the coating. In this study, we did not seek to increase the hydrophobicity of the coatings, since it is believed that the use of hydrophobic antifouling coatings does not help reduce the frictional resistance of the ship hull and marine equipment against water [30]. This statement is still as debatable, as the effect of hydrophobicity (and superhydrophobicity) on marine fouling.

The contact angle ( $\theta$ ) was measured using an LK-1 goniometer equipped with the Drop Shape computer program in compliance with the Russian standard 7934.2.

High adhesion and hardness are essential properties for marine coatings. The relative hardness of the coatings was found using a pendulum device (Persoz pendulum), in compliance with the Russian standard 52166.

The adhesion of the coatings was measured using an adhesion meter – by the method of lattice cuts, and was evaluated using a four-point system, in compliance with the Russian standard 15140.

The IR spectra of the initial components, sols, as well as coatings freshly deposited and aged in air for 1–2 days, were recorded using an FSM 2202 IR-Fourier spectrometer using a horizontal type multiple frustrated total internal reflection attachment – MATRT 36 in the frequency range of 4000–850  $\text{cm}^{-1}$ . The material of the MATRT prism was Ge.

For thermal analysis, we used the material of coatings obtained from sols of the above compositions, either DND-free or DND-modified. Some of the sols under study were subject to preliminarily evacuation and heating to 80 °C. A detailed description of experimental samples for thermal analysis is given in Table 1.

The thermal analysis was performed on a STA 429 CD synchronous thermal analysis unit from the German company NETZSCH using a platinum-platinum-rhodium sample holder of the “TG + DSC” type. To analyze the decomposition products, we also used a QMS 403 C quadrupole mass spectrometer from the same company, which made it possible to analyze thermal decomposition products in the range from 1 to 121 atomic charge units. The studies were carried out in an air flow (50  $\text{cm}^3\cdot\text{min}^{-1}$ ) with an increase in temperature from 40 to 1000 °C at a rate of 20 deg. per minute. To carry out the research, tablets weighing ~20 mg, 5 and 10 mm in diameter, and ~0.4–0.5 mm thick were pressed from the samples of composites under a pressure of ~1  $\text{kg}\cdot\text{mm}^{-2}$ .

**Table 1.** Research objects for thermal analysis

No.	DND content in a sol (by synthesis), wt. %	Pretreatment of the sol in a vacuum cabinet when heating, 80 °C, 2 h
1	–	–
2	–	+
3	0.4	–
4	0.4	+
5	0.2	–



### 2.3. Methodology of full-scale tests

The antifouling properties of visible-light-transparent coatings applied to magnifiers (as described above) were carried out on the basis of the Joint Russian-Vietnamese Research and Technology Tropical Center – in the coastal zone of the South China Sea (Nyachang).

Coated magnifiers were fixed on special stands, 5–6 pieces each. The stands were immersed to a depth of 2–3 m in the marine environment. After some time, intervals, dictated by different conditions (climatic, sea waves, etc.), stands were raised from sea water to assess the state of the surface of the plates. In our experiment, this was done on the 14th, 36th, 46th, 59th and 78th days after exposure to sea water. The types of the main marine foulers were determined. The degree of fouling was characterized as a percentage of the fouling area to the total surface area [31]. The study of experimental coatings was terminated when marine foulers occupied more than 50 % of the surface area.

## 3. Results and Discussion

### 3.1. Physico-mechanical properties of coatings

The physico-mechanical properties of epoxy-titanate coatings, both unmodified and DND-modified (contact angle, hardness, adhesion), were studied depending on different sol synthesis conditions (with preliminary evacuation of sol before coating deposition and without evacuation, as well as at room temperature and sample heating temperature

of 120 °C after coating) and coating methods (airbrushing and pouring).

Our studies have shown that the adhesion value was equally high for all coatings and was 1 point by Russian Standard 15140, which is the maximum value for this criterion.

The results of the study of the degree of hydrophilicity/hydrophobicity and hardness of the coatings are presented in Table 2.

As can be seen from Table 2, all coatings, regardless of the synthesis conditions and coating techniques, both DND-modified and non-DND-modified, are hydrophilic. The values of contact angles range from 51–80°. Non-DND modified coatings are characterized by a slight decrease in the contact angle as a result of additional heat treatment at 120 °C. This phenomenon is especially pronounced for a thinner coating applied under normal conditions with an airbrush from a non-evacuated sol before applying. The modification of DND coatings (from 0.2 to 0.4 wt. %) has virtually no effect on the contact angle when using an airbrush. However, when applied by pouring from a non-evacuated sol (i.e., when a somewhat thicker coating is formed), both without additional heat treatment and after it, a slight increase in the degree of hydrophobicity was observed upon the introduction of DND.

The hardness of the coatings significantly increased with DND modification. It is interesting to note that the hardness of coatings with a higher DND content (0.4 wt. %) was higher when preliminary

**Table 2.** Physico-chemical properties of coatings prepared under different conditions of sol synthesis and coating techniques

Coating techniques	Sol synthesis conditions*	Contact angle, deg.				Hardness, relative units		
		DND-free	DND, wt. %*		DND-free	DND, wt. %*		
			0.2	0.4		0.2	0.4	
Airbrushing	Outdoor	R.T.	74	60	64	0.3	0.9	0.8
		120 °C	54	60	67	0.4	0.9	0.8
	Vacuum	R.T.	60	52	55	0.3	0.8	0.9
		120 °C	56	53	54	0.4	0.8	0.9
Pouring	Outdoor	R.T.	55	73	72	0.1	0.9	0.8
		120 °C	54	76	78	0.2	0.9	0.8
	Vacuum	R.T.	57	56	80	0.1	0.8	0.9
		120 °C	56	51	79	0.2	0.8	0.9

\* R.T. – room temperature and non-evacuated; 120 °C – plate heating temperature after coating.

evacuation of the sols was used before coating deposition, while with a lower DND content (0.2 wt. %), on the contrary, it was higher when the sols were not pre-evacuated. Possibly, evacuation of the sol before coating causes its accelerated structure formation. Structural studies of compositionally identical sols based on TBT and EPONEX 1510, which we previously performed by the small-angle X-ray scattering (SAXS) method, made it possible to establish that evacuation at the aging stage of the sol promotes the formation of a fractal epoxy-titanate structure at the nanometer level, which, in turn, contributes to the strengthening of the structure [28]. In addition, the observed phenomenon is undoubtedly associated with the effect of DND on the structure of the emerging coating network. Thus, for epoxy-siloxane sols, small additions of DND (0.10–0.25 %) contribute to compaction and strengthening of the structure of the resulting coatings [12, 13, 27].

The coating technique affects only the relative hardness of DND-free coatings. At the same time, airbrushed coatings have greater hardness than poured coatings.

### 3.2. Evolution of the chemical composition of sols during their synthesis and aging

The hydrolysis of titanium alkoxides (TBT or titanium isopropoxide) underlies the production of both nanodispersed  $\text{TiO}_2$  as well as film-forming sols and thin transparent films based on them [32, 33]. AcAc is used as a complexing agent to reduce the high rate of hydrolysis that is characteristic of titanium alkoxides. This is especially important when it is necessary to obtain film-forming sols resistant to gelation and sedimentation. In the literature, there are studies devoted to the study of the hydrolysis of TBT, incl. in the presence of AcAc [32, 34], as well as TBT in combination with tetraethoxysilane and even with epoxy resin (bisphenol A diglycidyl ether) [5, 7]. At the same time, when studying the processes of hydrolysis and film formation in multicomponent organic-inorganic sols, it is necessary to take into account the influence of all sol components, not only precursors, but also solvents and hydrolysis and polymerization catalysts. In this study, using the method of IR spectroscopy, we examined and analyzed in detail (step by step) the processes occurring in a homogeneous medium of organic solvents (AcAc and ethyl cellosolve) during the formation of a sol based on TBT and hydrogenated epoxy resin, incl. in the presence of DND additives.

Figure 3 shows the IR spectra of the initial components of the investigated sols. Compared to the functional groups of the initial components inherent

in TBT and AcAc, their interaction produces bands at  $1584\text{ cm}^{-1}$  with a shoulder of  $1523\text{ cm}^{-1}$ , which are characteristic of the chelate ring (see Fig. 4), which indicates the formation of the complex compound  $[\text{Ti}(\text{OC}_4\text{H}_9)_{4-x}(\text{O}_2\text{C}_5\text{H}_7)_x]$  [34, 35, 36]. When TBT interacts with AcAs, butyl alcohol is formed – the absorption bands at  $3500$  and at  $1075$  and  $1024\text{ cm}^{-1}$  correspond to the stretching and bending vibrations of the OH group of butyl alcohol.

According to the IR spectra in Fig. 5, one can track the influence of the ethyl cellosolve solvent and an aqueous solution of  $\text{HNO}_3$ , which was supposed to initiate the process of hydrolysis of the titanium complex compound  $[\text{Ti}(\text{OC}_4\text{H}_9)_{4-x}(\text{O}_2\text{C}_5\text{H}_7)_x]$  formed as a result of the interaction of TBT with AcAc.

As can be seen from Fig. 5 (curve 2), the band of vibrations of bound OH groups becomes more intense. The bending vibrations of OH-groups related to alcohols ( $1064\text{ cm}^{-1}$ ) become wider and more intense. There are bond vibrations related to the C—O ( $1583\text{ cm}^{-1}$ ) and C—C ( $1530\text{ cm}^{-1}$ ) chelate ring, while there is a shift in the absorption band of the C—C bond vibration by  $7\text{ cm}^{-1}$  to a higher frequency region. Stretching asymmetric and symmetric vibrations of  $\text{CH}_3$ , stretching asymmetric vibrations of  $\text{CH}_2$ , bending vibrations of  $\text{CH}_2$  and  $\text{CH}_3$ , and stretching vibrations of C—O bonds are preserved. The shifts along these bands are almost invisible. There is a shift to the low-frequency region by  $10\text{ cm}^{-1}$  (from  $1124$  to  $1114\text{ cm}^{-1}$ ) of the absorption bands of vibrations of C—O—C and Ti—O—C bonds. Such a shift in the absorption bands of bond vibrations to high-frequency and low-frequency regions of the spectrum probably indicates the interaction of the intracomplex compound  $[\text{Ti}(\text{OC}_4\text{H}_9)_{4-x}(\text{O}_2\text{C}_5\text{H}_7)_x]$  with ethyl cellosolve to form the complex –  $[\text{Ti}(\text{OC}_4\text{H}_9)_{4-x-y}(\text{O}_2\text{C}_5\text{H}_7)_x(\text{OC}_2\text{H}_5)_y]$  [37].

The emergence of a characteristic absorption band at  $1717\text{ cm}^{-1}$  was due to the vibration of the C=O bond, probably related to the partially oxidized solvent, ethyl cellosolve [40].

As can be seen from Fig. 5 (curve 3), the addition of an aqueous acid solution did not cause significant changes in the composition of the solution: the shifts of the absorption bands were insignificant, and the emergence of new bands was not observed. Probably, the titanium acetylacetonate complex in the presence of ethyl cellosolve becomes more resistant to hydrolysis and subsequent polycondensation than the  $[\text{Ti}(\text{OC}_4\text{H}_9)_{3.617}(\text{O}_2\text{C}_5\text{H}_7)_{0.383}]$  complex [34].

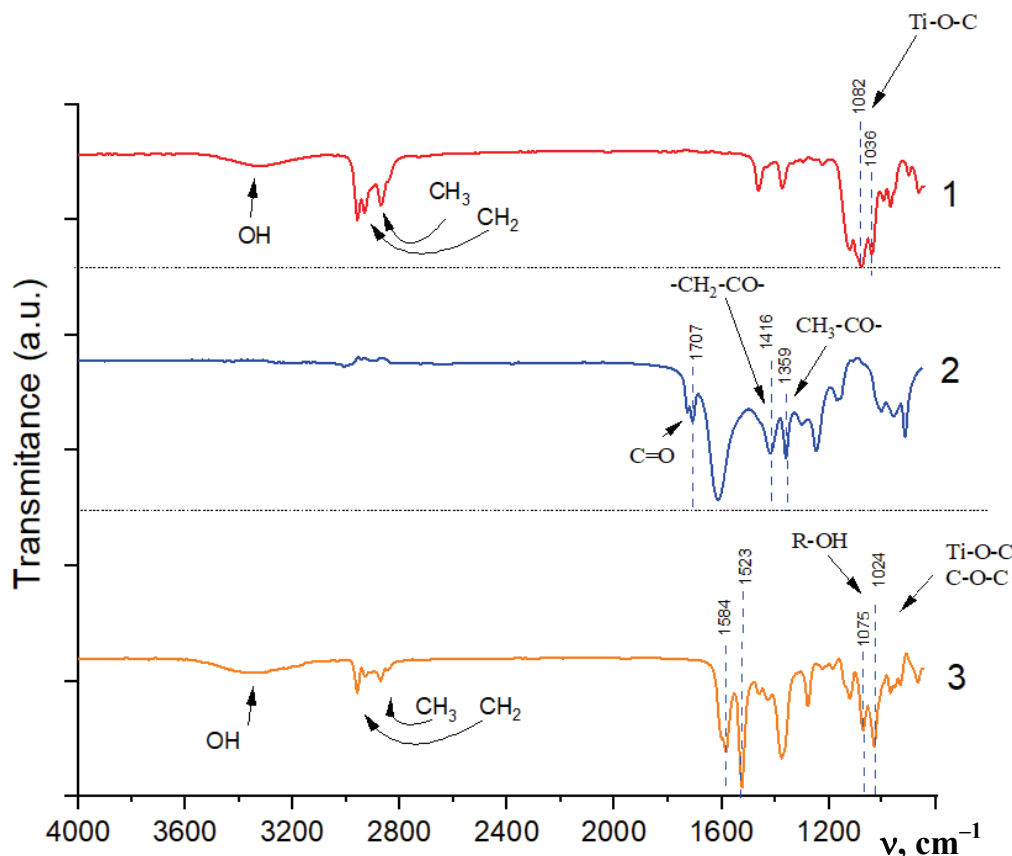


Fig. 3. FTIR spectra of the initial components of the organic-inorganic sol: TBT – 1, AcAc – 2 and their mixtures – 3

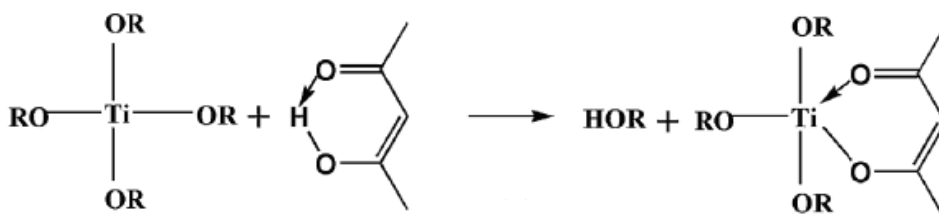


Fig. 4. The probable mechanism titanium complex compound formation in the interaction of TBT with AcAc

Figure 6 (curve 1) shows the IR spectrum of the Eponex 1510 epoxy resin. The absorption bands at 1251 and 906  $\text{cm}^{-1}$  belong to symmetric and asymmetric stretching vibrations of epoxy groups [39]. The deformation vibrations of the epoxy ring include vibrations below 850  $\text{cm}^{-1}$ ; they are not visible in the spectrum. Figure 6 (curve 2) shows the IR spectrum of an epoxy titanate sol based on uncured  $\text{BF}_3$  epoxy resin Eponex 1510 and an acetylacetone complex in ethyl cellosolve with an aqueous solution of nitric acid added. There are vibrations of OH-groups related to alcohols at 1284, 1067  $\text{cm}^{-1}$ . The vibrations of the C—O—C and Ti—O—C bonds remain unchanged at 1114  $\text{cm}^{-1}$ . The asymmetric stretching vibrations of the epoxy

group at 909  $\text{cm}^{-1}$  are still visible. In the IR spectra of the sol (Fig. 6, curve 3) prepared from the same composition, but with the addition of a catalyst for the cationic polymerization of epoxy resin (solution of  $\text{BF}_3$  in diethylene glycol), no changes were observed.

Figure 7 shows the IR spectra of organic-inorganic coatings prepared from the resulting epoxy-titanate sol. The evolution of the coating composition as the epoxy resin cures is traced. With exposure to air after the formation of the coating, the bands related to the vibrations of residual water, alcohol groups, and C=O groups completely disappear in the IR spectra, which can be associated with the evaporation of residual chemically unbound water

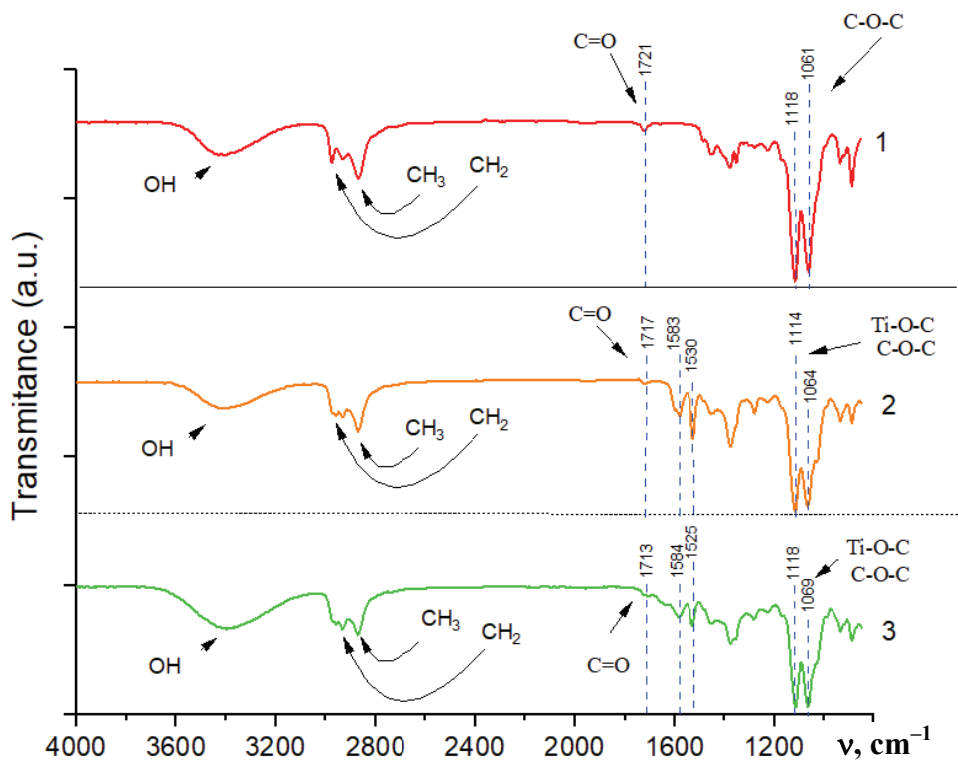


Fig. 5. FTIR spectra of intermediate solutions obtained by mixing a solution of TBT and AcAc with ethyl cellosolv – 2 and after adding  $\text{HNO}_3$  (0.1 N) – 3 to it, in comparison with the spectrum of ethyl cellosolv – 1

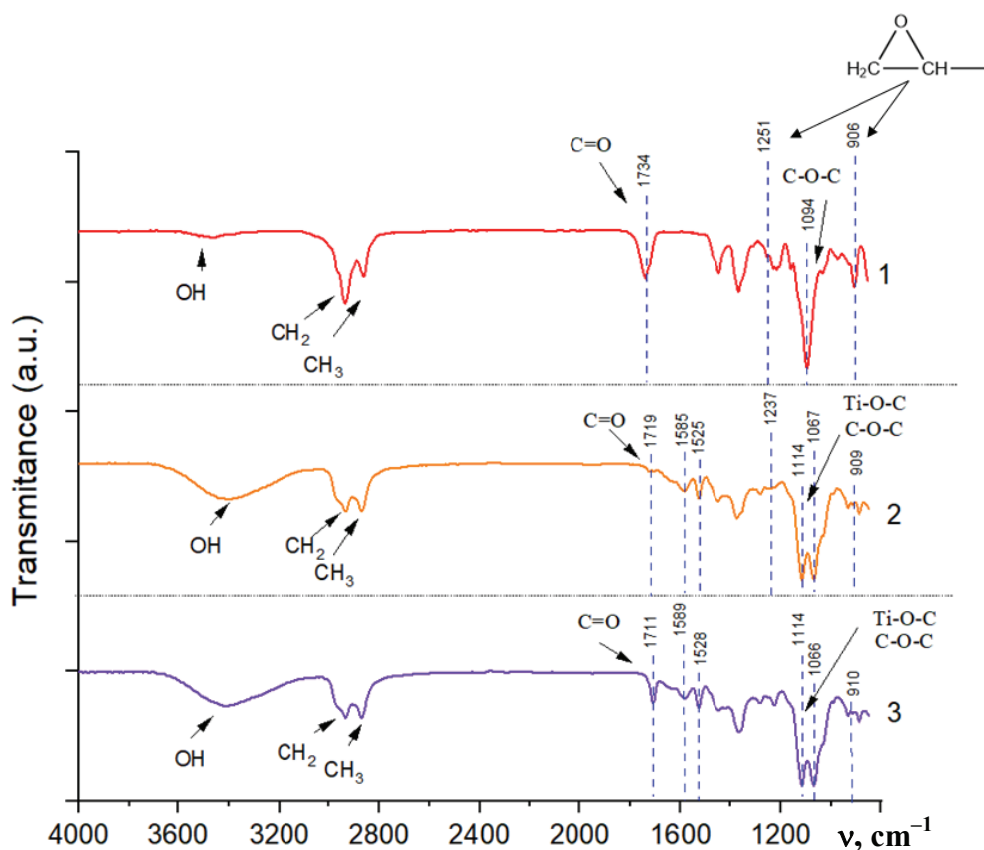


Fig. 6. FTIR spectra of the epoxy resin Eponex 1510 – 1; after mixing the epoxy resin with a solution of TBT in AcAc and ethyl cellulose – 2; the resulting solution – after adding  $\text{BF}_3$  in diethylene glycol – 3



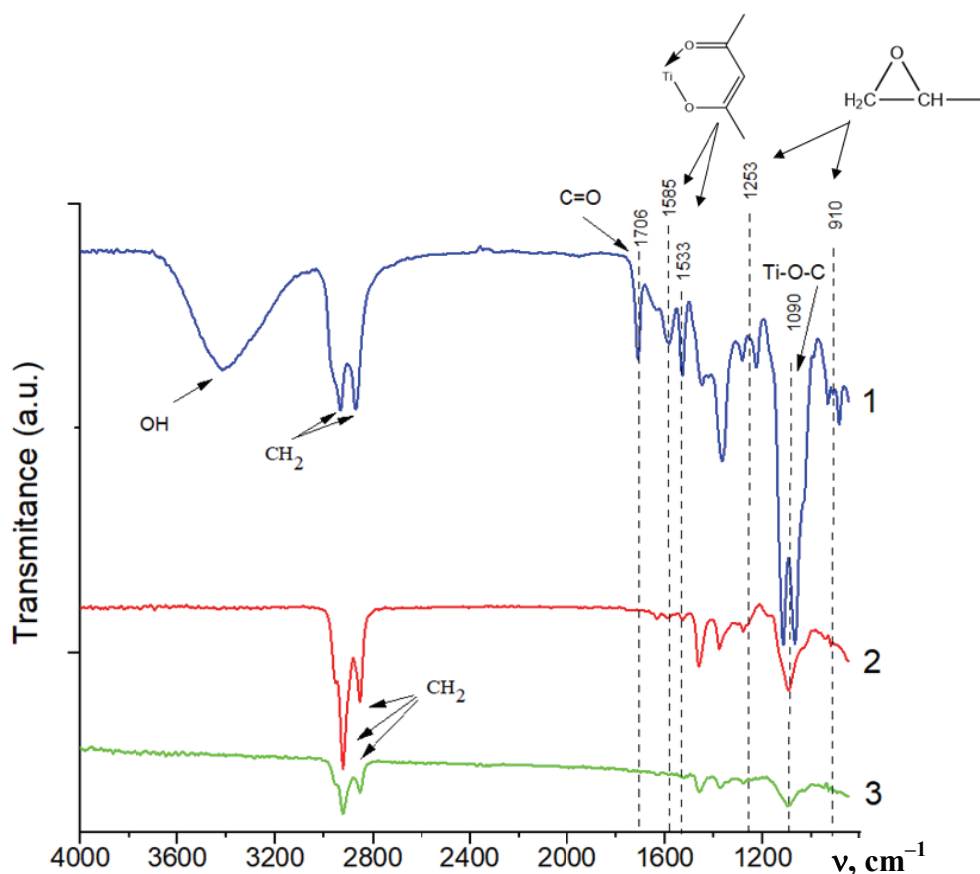


Fig. 7. FTIR spectra of organic-inorganic coatings 10 minutes after application and after exposure to air for 1 and 2 days

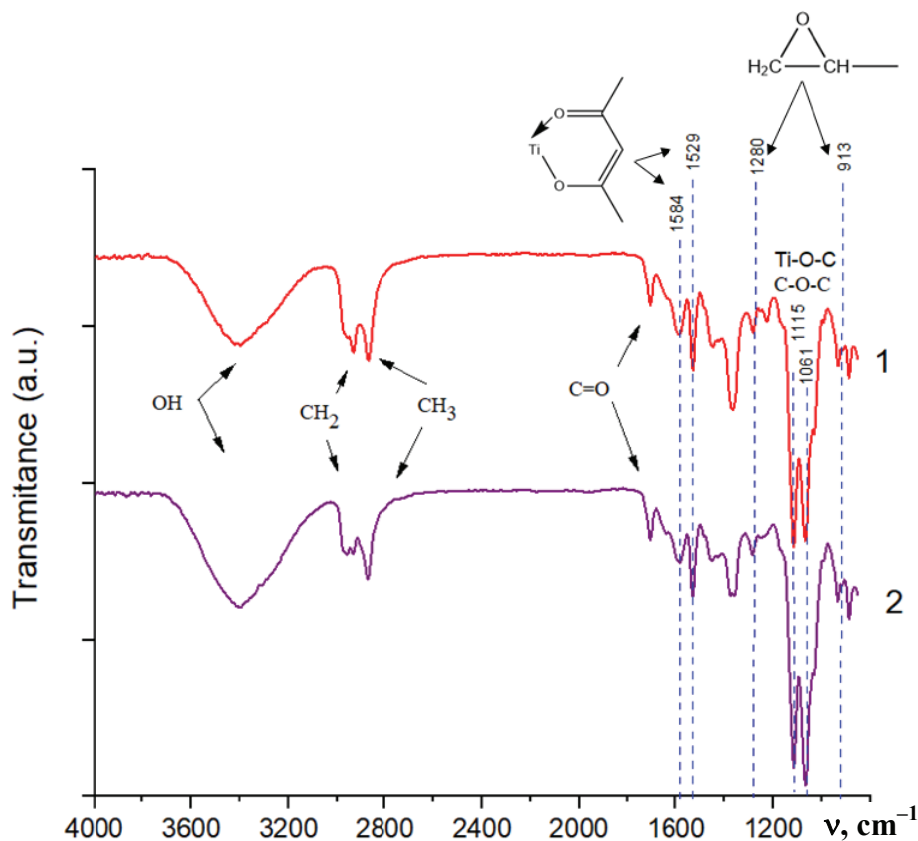


Fig. 8. FTIR spectra of epoxy-titanate coatings taken 10 minutes after coating sols without DND (1) and with DND (0.4 wt. %) – 2

and organic solvents, i.e. with drying coating. The epoxy rings are completely opened, as evidenced by the disappearance of the bands at 920 and 872  $\text{cm}^{-1}$ , and the bands characteristic of the Ti—O—C chelate ring (1585 and 1533  $\text{cm}^{-1}$ ) become less intense.

This indicates the formation of a cross-linked polymer structure of the composite coating based on epoxy resin and TBT. It was of interest to study the effect of DND on the composition of the resulting coatings prepared from DND-modified sols (0.4 wt. %) (Fig. 8).

Figure 8 shows that DND did not have a significant effect on chemical interactions in the sol, only the peak belonging to OH vibrations increases, since DND was introduced into the sol in the form of an aqueous suspension. As is known, DND is a structuring agent that affects the supramolecular structure of sols and coatings [13, 40]. At the same time, apparently, it does not enter into chemical reactions with the components of the epoxy-titanate sol.

### ***3.3. Evolution of the chemical composition of coatings during heat treatment***

The physico-mechanical properties and thermal stability of coatings are significantly affected by the conditions of their formation. In our case, this is evacuation of the sol at an elevated temperature before coating and/or modification of the DND epoxy coating (with a DND content in sols of 0.2 or 0.4 wt. %, according to synthesis). In addition, during the operation of coatings, it is important to know the thermal and thermal-oxidative stability of coatings in air. Therefore, a thermal analysis of the coating material was performed. In addition, the results of thermal analysis make it possible to indirectly characterize the composition of the resulting coatings.

During the thermal analysis, changes in the mass of the sample in % of the sample size (curve TG), differential curve TG (curve DTG) and changes in enthalpy accompanying thermal transformations (curve DSC) were measured simultaneously. Also, curves of changes in the values of ion currents (curves IC) due to different masses of ions in the products of thermal decomposition were obtained.

Thermal analysis curves for TG, DTG, and DSC combined with IC mass spectrometric analysis (ion current due to ions with a mass of 18.44) are shown in Figs. 9–11.

Figure 9 shows the effect of preliminary evacuation (when sols are heated to 80 °C) on DND-free coatings. As was shown earlier (see Section 3.1,

Table 2), this technique affected the physico-mechanical properties of DND-free coatings.

Analyzing the curves in Fig. 10, it is possible to evaluate the effect of preliminary evacuation and heating of sols on thermal effects in coatings containing the same amount of DND in sols (0.4 wt. %).

Studying the thermal effects in Fig. 11, it is possible to establish the effect of changing the DND concentration in sols from 0.2 to 0.4 wt. %. The preliminary evacuation and heating of the sols were not performed in this case.

In general, analyzing Figs. 9–11, it can be concluded that the physico-chemical processes accompanying the thermal-oxidative degradation of epoxy-titanate coatings under non-isothermal conditions with the access of atmospheric oxygen proceed in several stages. At the first stage, the studied coatings are characterized by the appearance of weak broad endothermic peaks on the DSC curves due to the removal of chemically unbound volatile components (water, organic solvents, unreacted sol components). The second stage refers to the carbonization of the organic part of the composites [5–8, 14]. At this stage, it is possible to distinguish the temperature interval where an intense mass loss occurs. In this temperature range, processes occur that are accompanied by an exothermic effect and a large loss of mass associated with the burnout of the organic component. At the third stage, carbon (coke) burns out, accompanied by exothermic processes and a relatively small weight loss. At this stage, one can distinguish temperature intervals with a noticeable heat release, but with a small loss of mass. The sharp maximum of the complex exo-effect at the second stage and the maximum of the exo-effect at the third stage coincide with the corresponding two maxima on the differential curves for the yield of volatile products (both carbon dioxide and water). This coincidence indicates that the carbonization of the epoxy-titanate coating proceeds in two stages.

A detailed analysis of the thermal characteristics for these coatings during their heating is given in Tables 3–5.

As can be seen from Table 3, preliminary evacuation and slight heating of the sols up to 80 °C affect the course of thermal processes in the coating material. Significantly less weight loss was observed in evacuated and heated samples in the temperature range from RT to 180 degrees. For heated and evacuated samples, the maxima of exothermic effects associated with carbonization processes, especially at the 3rd stage, are shifted towards higher temperatures, which proceed with a significantly

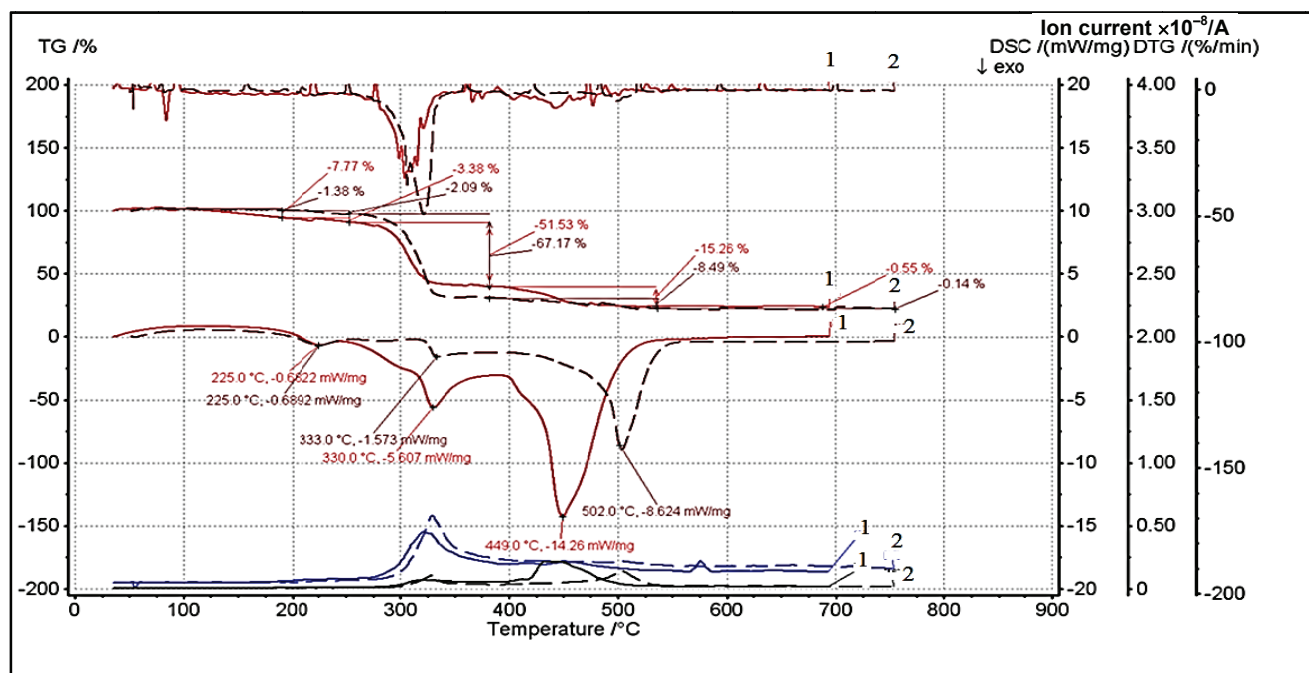


**Fig. 9.** TG, DTG and DSC curves for epoxy-titanate DND-free coatings (see Table 1): from the non-evacuated sol (red solid line – 1) and pre-evacuated sol at 80 °C (brown dashed line – 2).

At the bottom of the Figure there are the IC volatile release curves:

Water (mass number 18 a.m.u.): upper blue solid line (1); upper blue dashed line (2).

Carbon dioxide (mass number 44 a.m.u.): bottom black solid line (1); bottom black dashed line (2)

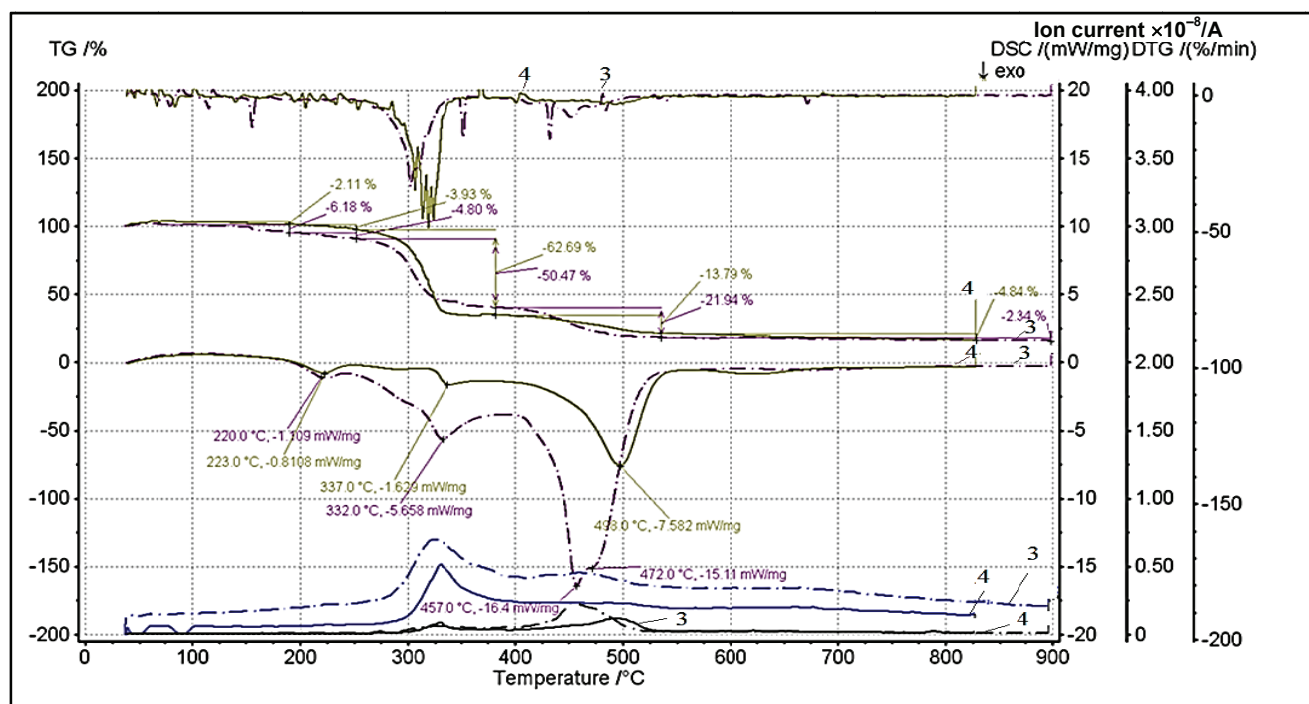


**Fig. 10.** TG, DTG, and DSC curves for epoxy-titanate coatings containing the same amount of DND, 0.4 wt. % (see Table 1): preliminary evacuated and heated sol (purple dashed-dotted line – 3) nonevacuated or heated to 80 °C (green solid line – 4).

At the bottom of the Figure there are the IC volatile release curves:

Water (mass number 18 a.m.u.): upper blue dashed-dotted line (3) and upper blue solid line (4).

Carbon dioxide (mass number 44 a.m.u.): bottom black dashed-dotted line (3) and bottom black solid line (4)

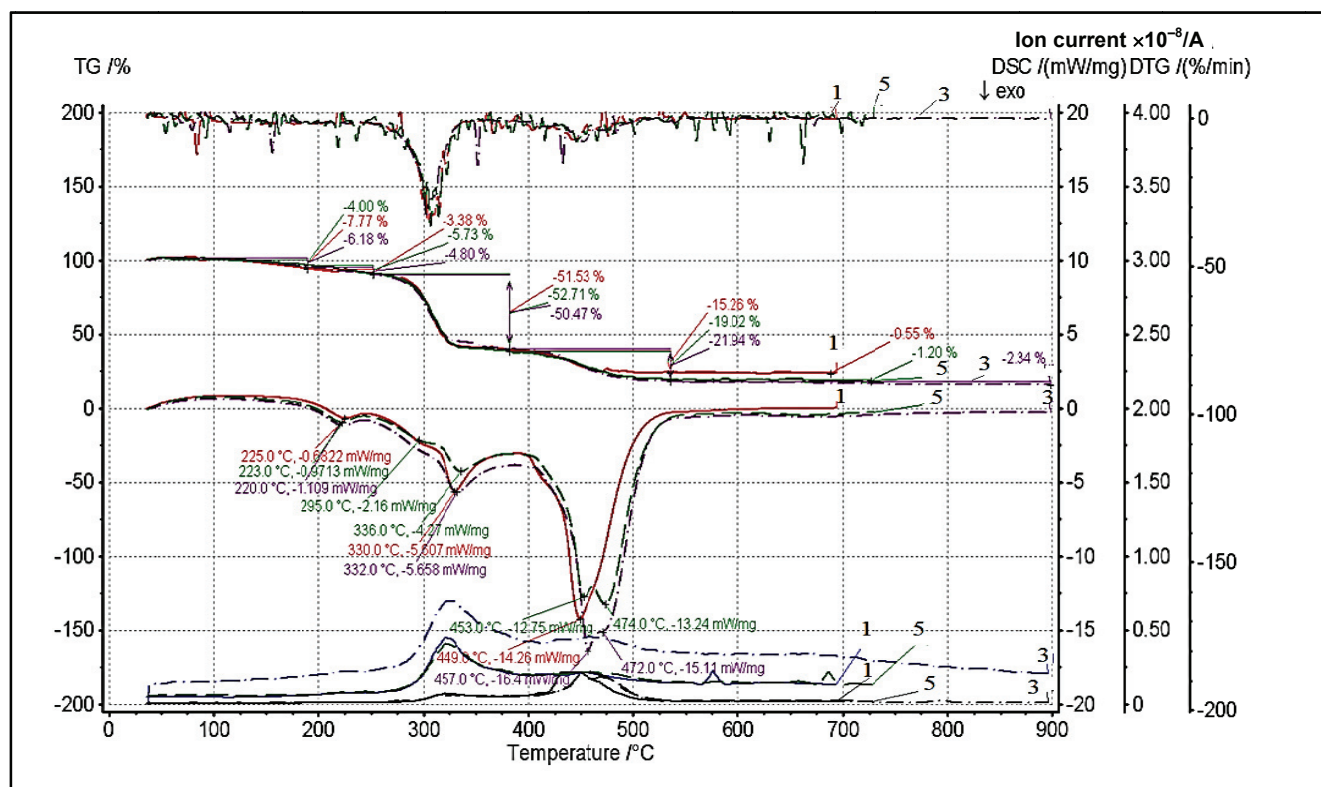


**Fig. 11.** TG, DTG, and DSC curves for epoxy-titanate coatings: without DND (red solid line – 1) and containing various amounts of DND: 0.2 wt. % (green dashed line – 5) and 0.4 wt. % (purple dashed-dotted line – 3).

At the bottom of the figure are the IC volatile release curves:

Water (mass number 18 a.m.u.): upper blue solid line (1), upper green dashed line (5) and upper blue dashed-dotted line (3).

Carbon dioxide (mass number 44 a.m.u): black solid line (1), black dashed line (5) and black dashed-dotted line (3)

**Table 3.** Thermal characteristics of DND-free epoxy-titanate coatings prepared from pre-evacuated and heated sols and non-evacuated sols

Characteristics		Additional acting on sols		Characteristics change, $\pm\Delta$
		No evacuation or heating	Evacuation and heating to 80 °C	
Temperature range, °C:	Max on DSC curve, °C	Weight loss $\Delta m$ , %		
Stage 1: RT-180	Weak and diffused	7.8	1.4	-6.4
Stage 2: 180–375	225, 300, 330 225, –, 333	54.7	69.3	+14.6
Stage 3: 375–700	449 502	15.8	8.6	-7.2
Total weight loss		78.3	79.3	+1.0
Max on mass spectrometric curves		Temperature, °C		
Water:				
$I_{\max}$ on the ion current curve		~320	450	+130
$II_{\max}$ on the ion current curve		~325	very weak effect ~500	+175
Carbon:				
$I_{\max}$ on the ion current curve		~325	~325	0
$II_{\max}$ on the ion current curve		~450	~500	+50



**Table 4.** Thermal characteristics of epoxy-titanate coatings prepared from sols containing DND 0.4 wt. %, prepared from sols with preliminary evacuation and heating and without these effects

Characteristics		Additional acting on sols		Characteristics difference
		No effects	Evacuation and heating to 80 °C	
Temperature range, °C:	Max on DSC curve, °C:	Weight loss $\Delta m$ , %		
Stage 1: RT-180	—	6.8	2.1	−4.7
Stage 2: 180–375	220, 332 223, 337	66.6	55.3	−11.3
Stage 3: 375–830	474 493	24.3	18.6	−5.7
Total weight loss		97.7	76	−21.7
Max on mass spectrometric curves		Temperature, °C		
Water:				
$I_{\max}$ on the ion current curve		~325	~330	+5
$II_{\max}$ on the ion current curve		~470	very weak effect ~500	+30
Carbon:				
$I_{\max}$ on the ion current curve		~330	~330	0
$II_{\max}$ on the ion current curve		~460	~490	+30

**Table 5.** Thermal characteristics of epoxy-titanate DND-free coatings and coatings containing different amounts of DND prepared from sols without preliminary evacuation and heating

Characteristics		DND content in sols, wt. %			Characteristics difference
		0	0.2	0.4	
Temperature range, °C:	Max on DSC curve, °C:	Weight loss, $\Delta m$ , %			
Stage 1: RT-180	–	7.8	4.0	6.2	–3.8 –1.6
Stage 2: 180–375	225, 295, 330 223, – 336 220, – 332	54.8	58.7	55.9	+3.9 +1.1
Stage 3: 380–900	449 453, 474 472	15.8	20.2	23.6	+4.4 +7.2
Total weight loss		78.4	82.9	85.7	+4.5 +7.3
Water:					
$I_{\max}$ on the ion current curve		~325	~325	~330	0 +5
$II_{\max}$ on the ion current curve		~450	~450	~460	0 +10
Carbon:					
$I_{\max}$ on the ion current curve		~325	~325	~325	0 0
$II_{\max}$ on the ion current curve		~450	~470	~450	+20 0

lower heat release, and the evaporation of vapors of chemically bound water, which is usually removed from materials at high temperature ( $\geq 500^\circ\text{C}$ ), is practically absent. In this case, the total weight loss for both options is almost the same. Based on these data and the physico-mechanical properties of the coatings (see Table 2), it can be concluded that evacuation in combination with heating and, apparently, especially heating to  $80^\circ\text{C}$ , lead to coating densification, which does not contradict traditional ideas about sol-gel materials during heat treatment.

The modification of the coating material with a small amount of DND (0.4 wt. % in sol, according to synthesis) changed the nature of the occurrence of thermal processes in the coating material – see Table. 4. The total weight loss of the samples prepared from the sol without evacuation and heating was much greater. For the same samples, two peaks appeared on the curve illustrating the process of water release. This can be associated with the DND effect, which is characterized by the ability to intensify the hydration processes of various materials [12, 40]. The temperature maxima shifted towards

higher temperatures at all stages of the degradation processes and subsequent carbonization. In this case, preliminary evacuation and slight heating of the sols (up to  $80^\circ\text{C}$ ) ensured significantly lower mass losses due to the removal of water, both physically and chemically bound. The total weight loss slightly increased when the coating material was modified with small additions of DND (0.2 and 0.4 wt. %, according to synthesis) (Table 5). The exo-effects for DND-coated coating materials had a complex shape, indicating a multi-stage thermal decomposition process. The temperature maxima of the exothermic effects slightly shifted towards higher temperatures. An increase in the DND content within the indicated limits had practically no effect on the course of thermal degradation and carbonization processes.

### 3.4. Antifouling properties of coatings

It is known [21, 28, 41, 42] that DND has a mild bactericidal and fungicidal effect, inhibiting the development of pathogenic bacteria and fungi. The results of the study of the antifouling activity of DND-modified epoxy-titanate coatings are shown in Fig. 12.

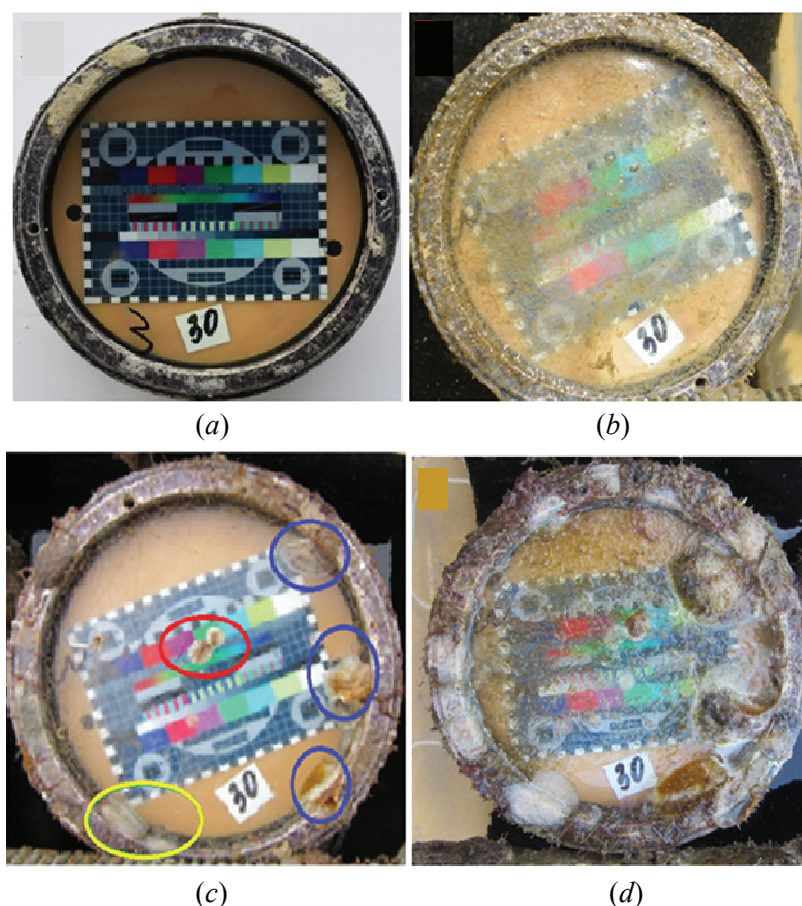


**Fig. 12.** Optical images of an experimental coating prepared from a sol based on hydrolyzed TBT and an epoxy resin modified with DND 0.2 wt. %:  
a – after installation at sea; b – after 14 days; c – 59 days; d – 78 days after installation

After about 14 days of being in the water, a bacterial film appeared; it serves as the basis for the attachment and nutrition of marine foulers. At the same time, its presence is an indicator that the coating is not toxic. 33 days after the dive, no signs of fouling were detected. Foulers began to appear after 45 days in sea water, but in small numbers. After 59 days, an increase in macrofouling was recorded to varying degrees by different types of foulers. After 78 days the foulers occupied a little more than 50 % of the total surface area. This percentage is a signal to stop further research. During this period, the following marine foulers were discovered: oysters, balanus, bryozoans, serpulids. For the use of "soft biocides" a period of 78 days is good enough. Research in this direction is ongoing.

#### 4. Conclusions

Sedimentation and kinetically stable film-forming epoxy-titanate sols were synthesized using the methods of sol-gel technology, starting from EPONEX 1510 aliphatic epoxy resin and a solution of tetrabutoxytitanium in acetyl acetone and ethyl cellosolve, in the presence of an aqueous solution of nitric acid and a catalyst for the cationic polymerization of BF<sub>3</sub> epoxy resin.

It was shown by IR spectroscopy that weakly hydrolyzable titanium intracomplex compounds are gradually formed in the sols. For a more complete opening of epoxy rings and the formation of a polymeric structure of coatings, exposure to air at room temperature for at least 1–2 days is necessary.

Transparent epoxy-titanate coatings prepared by pouring or airbrushing on the surface of optical glass substrates are hydrophilic and have good adhesion to the glass surface (1 point according to Russian Standard 15140). Modification of the epoxy titanate sol with a small amount of detonation nanodiamond (0.2 and 0.4 wt. % DND) reduces the degree of hydrophilicity of the coatings and significantly increases the relative hardness of the coatings (from 0.1–0.4 to 0.8–0.9, according to Russian Standard 52166).

The method of applying coatings by airbrushing or pouring, other things being equal, does not affect the relative hardness of DND-modified coatings, but does affect the relative hardness of DND-free coatings, applied by airbrush, which have a higher relative hardness than coatings applied by pouring.

The results of thermal analysis, coupled with the study of physico-mechanical properties, enable to state that preliminary evacuation and heating of the sols to 80 °C, as well as the addition of DND, contribute to the densification of the structure of the

coating material and increase their thermal stability. In addition, the introduction of DND into the sols intensifies the hydration processes in the sols.

Marine field tests in tropical sea conditions of transparent antifouling epoxy-titanate coatings obtained from sols modified with 0.2 wt. % DND (by synthesis) deposited on glass surfaces showed that DND can be considered as a mild biocide or synergist that weakly inhibits the process of marine fouling.

#### 5. Funding

The synthesis of sols and coatings and laboratory studies of their properties were conducted as part of the research project 0081-2022-0006; marine full-scale tests were conducted by the Russian-Vietnamese Research and Technological Tropical Center.

#### 6. Conflict of interests

The authors declare no conflicts of interest.

#### References

1. Ruggiero L, Fidanza MR, Iorio M, Tortora L, Caneva G, Ricci MA, Sodo A. Synthesis and characterization of TEOS coating added within innovative antifouling silica nano containers and TiO<sub>2</sub> nanoparticles. *Frontiers in Materials*. 2020;7:185. DOI:10.3389/fmats.2020.00185
2. Liang Y, Sun S, Deng T, Ding H, Chen W, Chen Y. The preparation of TiO<sub>2</sub> film by the sol-gel method and evaluation of its self-cleaning property. *Materials*. 2018;11(3):450. DOI:10.3390/ma11030450
3. Litter MI, Vera ML, Traid HD. TiO<sub>2</sub> coatings prepared by sol-gel and electrochemical methodologies. In: Almeida R, Martucci A, Santos L, Rocío Estefanía Rojas Hernández (eds) *Sol-Gel Derived Optical and Photonic Materials. Series in Electronic and Optical Materials*. Woodhead Publishing; 2020. p. 39-74. DOI:10.1016/C2018-0-02962-X
4. Guo F, Gao J, Li X. Research progress on titanium-containing organic-inorganic hybrid protective coatings. *Surface Review and Letters*. 2019;26(9):1930002. DOI:10.1142/S0218625X19300028
5. Lyga RI, Mikhalechuk VM. Epoxy composites containing silica and titanium dioxide *Vestnik Voronezhskogo Gosudarstvennogo Universiteta. Seriya: Khimiya. Biologiya. Farmatsiya* 2021;3:17-25. (In Russ.).
6. Cardiano P, Sergi S, Lazzari M, Piraino P. Epoxy-silica polymers as restoration materials. *Polymer*. 2002; 43(25):6635-6640. DOI:10.1016/S0032-3861(02)00677-8
7. Lu S, Zhang H, Zhao C, Wang X. New epoxy/silica-titania hybrid materials prepared by the sol-gel process. *Applied Polymer Science*. 2006;101(2):1075-1081. DOI:10.1002/app.23742
8. Zhil'tsova SV, Mikhalechuk VM, Beloshenko VA, Kirilash AV. Influence of the molar ratio of



tetraethoxysilane and glycidoxypolytriethoxysilane on the properties of anhydride-cured epoxy-siloxane composites. *Russian Journal of Applied Chemistry*. 2009;82(4):673-679. DOI:10.1134/S1070427209040247

9. Alyamac E, Gu H, Soucek MD, Qiu S, Buchheit RG. Alkoxysilane oligomer modified epoxide primers. *Progress in Organic Coatings*. 2012;74(1):67-81. DOI:10.1016/j.porgcoat.2011.11.012

10. Torrico Ruben FAO, Harb SV, Trentin A, Uvida MC, Pulcinelli SH, Santilli CV, Hammer P. Structure and properties of epoxy-siloxane-silica nanocomposite coatings for corrosion protection. *Journal of Colloid and Interface Science*. 2018;513:617-628. DOI:10.1016/j.jcis.2017.11.069

11. Movchan TG, Khamova TV, Shilova OA, Plachev YuA, Sokolova NP, Gorbunov AM, Sazhnikov VA. Influence of the composition and structure of epoxy siloxane matrix on the spectral behavior of the Nile red dye: I. Sol-gel system based on tetraethoxysilane and a mixture of epoxy resins. *Glass Physics and Chemistry*. 2009;35(1):87-93. DOI:10.1134/s1087659609010131

12. Khamova TV, Shilova OA, Kopitsa GP, Almásy L, Rosta L. Small-angle neutron scattering study of the mesostructure of bioactive coatings for stone materials based on nanodiamond-modified epoxy siloxane sols. *Physics of the Solid State*. 2014;56(1):105-113. DOI:10.1134/S1063783414010156

13. Khamova TV, Shilova OA, Kopitsa GP, Angelov BA, Zhigunov A. Effect of biocidal additives on the mesostructure of epoxy-siloxane bioactive coatings. *Journal of Surface Investigation*. 2016;10(1):113-122. DOI:10.1134/S1027451015060312

14. Burmistrov IN, Mostovoi AS, Panova LG, Shatrova NV, Kuznetsov DV, Il'Inykh IA, Gorokhovskii AV. Influence of surface modification of potassium polytitanates on the mechanical properties of polymer composites thereof. *Russian Journal of Applied Chemistry*. 2013;86(5):765-771. DOI:10.1134/S107042721305025X

15. Bakhshandeh E, Jannesari A, Ranjbar Z, Sobhani S, Saeb MR. Anti-corrosion hybrid coatings based on epoxy-silica nano-composites: toward relationship between the morphology and EIS data. *Progress in Organic Coatings*. 2014;77(7):1169-1183. DOI:10.1016/j.porgcoat.2014.04.005

16. Nazir T, Afzal A, Siddiqi HM, Ahmad Z, Dumon M. Thermally and mechanically superior hybrid epoxy-silica polymer films via sol-gel method. *Progress in Organic Coatings*. 2010;69(1):100-106. DOI:10.1016/j.porgcoat.2010.05.012

17. Shilova OA, Khamova TV, Mikhal'chuk VM, Vlasov DY, Dolmatov VYu, Frank-Kamenetskaja OV, Marugin AM. *Composition for making biologically stable coating*. Russian Federation patent 2,382,059. 20 February 2010.

18. Kobayashi M, Saito H, Boury B, Matsukava K, Sugahara Y. Epoxy-based hybrids using TiO<sub>2</sub> nanoparticles via a non-hydrolytic sol-gel rout. *Applied Organometallic Chemistry*. 2013;27(11):673-677. DOI: 10.1002/aoc.3027

19. Skopintseva NB, Indeikin YeA. The influence of titanium dioxide on internal stresses of formed epoxy

coatings. *Izvestiya Vysshikh Uchebnykh Zavedeniy. Seriya: Khimiya i Khimicheskaya Tekhnologiya* = *ChemChemTech*. 2007;50(4):87-90. (In Russ.).

20. Kausar A. Nanodiamond reinforced epoxy composite: prospective material for coatings Ch. 9. In: Liang Li, Qing Yang (eds.) *Advanced Coating Materials*. WILEY-Scrivener Publisher; 2018. p. 255-274. DOI:10.1002/9781119407652.ch9

21. Dolmatov VYu. Detonation-synthesis nanodiamonds: synthesis, structure, properties and applications. *Russian Chemical Reviews*. 2007;76(4):339-360. DOI:10.1070/RC2007v076n04ABEH003643

22. Voznyakovskii AP. Self-organization in nanocomposites based on detonation nanodiamonds. *Physics of the Solid State*. 2004;46(4):644-648. DOI:10.1134/1.1711441

23. Gavrilov AS, Voznyakovskii AP. Rheological characteristics and relaxation properties of polymer-nanodiamond composites. *Russian Journal of Applied Chemistry*. 2009;82(6):1041-1045. DOI:10.1134/S1070427209060214

24. Pramatarova L, Radeva E, Pecheva E, Hikov T, Krasteva N, Dimitrova R, Mitev D, Montgomery P, Sammons R, Altankov G. The advantages of polymer composites with detonation nanodiamond particles for medical applications. Ch. 14. In: L. Pramatarova (ed.) *On Biomimetics*. InTech; 2011. 656 p. DOI:10.5772/22903

25. Voznyakovskii AP, Prokoshev AO. Model of polymer reinforcement with detonation nanodiamonds. *Journal of Macromolecular Science. Part B: Physics*. 2013; 52(12):1811-1817. DOI:10.1080/00222348.2013.808882

26. Nezamdoust S, Seifzadeh D, Habibi-Yangjeh A. Nanodiamond incorporated sol-gel coating for corrosion protection of magnesium alloy. *Transactions of Nonferrous Metals Society of China*. 2020;30(6):1535-1549. DOI:10.1016/S1003-6326(20)65317-1

27. Shilova OA. Synthesis and structure features of composite silicate and hybrid TEOS-derived thin films doped by inorganic and organic additives. *Journal of Sol-Gel Science and Technology*. 2013;68:387-410. DOI:10.1007/s10971-013-3026-5

28. Shilova OA, Vlasov DY, Zelenskaya MS, Ryabusheva YV, Khamova TV, Glebova IB, Sinelnikov AA, Marugin AM, Frank-Kamenetskaya OV. Sol-gel derived TiO<sub>2</sub> and epoxy-titanate protective coatings: Structure, property, fungicidal activity and biomineralization effects. Ch. 33. In: Frank-Kamenetskaya OV, Vlasov DY, Panova EG, Lessovaia SN. (eds.). *Lecture Notes in Earth System Sciences*. Springer Cham; 2020. p. 619-638. DOI:10.1007/978-3-030-21614-6\_33

29. Zherebtsov DA, Kolmogortsev AM, Viktorov VV, D'yachuk VV, Galimov DM, Serikov AS, Mikhailov GG. Synthesis of nanosized titanium dioxide from tetrabutoxytitanium. *Russian Journal of Inorganic Chemistry*. 2010;55:1850-1856. DOI:10.1134/S0036023610120065

30. Orlov O, Sverchkov A. Assessing the possibility of applying hydrophobic coatings to reduce hydrodynamic resistance of cargo carriers. *Trudy Krylovskogo*



gosudarstvennogo nauchnogo tsentra = Transactions of the Krylov State Research Centre. 2018;383(1):43-59. DOI:10.24937/2542-2324-2018-1-383-43-59 (In Russ.).

31. Karpov VA, Koval'chuk YL, Poltarukha OP, Il'in IN. *Integrated approach to protection against marine growth and corrosion*. Moscow: Publishing House Association of Scientific Publications KMK; 2007. 156 p. (In Russ.).

32. Zherebtsov DA, Viktorov VV, Kulikovskikh SA, Belaya EA, Galimov DM. Synthesis of nanoparticulate anatase sol from tetrabutoxytitanium. *Inorganic Materials*. 2016;52(1):33-37. DOI:10.1134/S0020168516010167

33. Shapovalov VI, Shilova OA, Smirnova IV, Zav'yalov AV, Lapshin AE, Magdysyuk OV, Panov MF, Plotnikov VV, Shutova NS. Modification of the glass surface by titanium dioxide films synthesized through the sol-gel method. *Glass Physics and Chemistry*. 2011;37(2):150-156. DOI:10.1134/S1087659611020143

34. Simonenko NP, Nikolaev VA, Simonenko EP, Sevastyanov VG, Kuznetsov NT. Influence of the composition of  $[\text{Ti}(\text{OC}_4\text{H}_9)_{4-x}(\text{O}_2\text{C}_5\text{H}_7)_x]$  complexes and hydrolysis conditions on the synthesis of titania by sol-gel technology. *Russian Journal of Inorganic Chemistry*. 2016;61(8):929-939. DOI:10.1134/S0036023616080167

35. Tarasevich BN. *IR spectra of the main classes of organic compounds. Reference materials*. Moscow: Lomonosov Moscow State University publ.; 2012. 55 p. (In Russ.).

36. Zhou C, Ouyang J, Yang B. Retarded hydrolysis-condensing reactivity of tetrabutyl titanate by acetylacetone and the application in dye-sensitized solar cells. *Materials Research Bulletin*. 2013;48:4351-4356. DOI:10.1016/j.materresbull.2013.07.016

37. Isirikyan AA, Mikhailova SS, Polunina IA, Tolstaya SN. Modification of the titanium dioxide surface by aliphatic carboxylic acids. *Bulletin of the Academy of Sciences of the USSR. Division of Chemical Sciences*. 1983;32(1):12-16. DOI:10.1007/BF01167751

38. Kuzhel' AV, Puchkov SV, Vanin VV, Perkel AL. Features of liquid-phase oxidation of ethylcellulose. *Vestnik Kuzbasskogo Gosudarstvennogo Tekhnicheskogo Universiteta*. 2010;4(80):104-106. (In Russ.).

39. Yin Q, Yang W, Sun C, Di M. Preparation and properties of lignin-epoxy resin composite. *Bio Resources*. 2016;7(4):5737-5748. DOI:10.15376/biores.7.4.5737-5748

40. Shilova OA, Frank-Kamenetskaya OV, Korobkova AI. On the influence of detonation nanodiamond dopants on phase content and hydration features of portland cement materials. *Glass Physics and Chemistry*. 2015;41(2):206-211. DOI:10.1134/S108765961502011X

41. Shilova OA, Tsvetkova IN, Vlasov DY, Ryabusheva YV, Sokolov GS, Kychkin AK, Nguyen van C, Khoroshavina YV. Microbiologically induced deterioration and environmentally friendly protection of wood products. Ch. 13. In: Hafiz MN Iqbal, Muhammad Bilal, Tuan Anh Nguyen, Ghulam Yasin (eds.). *Biodegradation and Biodeterioration at Nanoscale*. Elsevier Inc; 2022. p. 283-321. DOI:10.1016/B978-0-12-823970-4.00013-0

42. Shilova OA, Vlasov DY, Khamova TV, Zelenskaya MS, Frank-Kamenetskaya OV. Microbiologically induced deterioration and protection of outdoor stone monuments. Ch.15. In: Hafiz MN Iqbal, Muhammad Bilal, Tuan Anh Nguyen, Ghulam Yasin (eds.). *Biodegradation and Biodeterioration at Nanoscale*. Elsevier Inc; 2022. p. 339-367. DOI:10.1016/B978-0-12-823970-4.00015-4

## Information about the authors / Информация об авторах

**Olga A. Shilova**, D. Sc. (Chem.), Professor, Chief Researcher, Institute of Silicate Chemistry of Russian Academy of Sciences, St. Petersburg, Russian Federation; Professor of the Basic Department of St. Petersburg State Electrotechnical University "LETI", St. Petersburg, Russian Federation; ORCID 0000-0002-3856-9054; e-mail: olgashilova@bk.ru

**Irina B. Glebova**, Researcher, Institute of Silicate Chemistry of Russian Academy of Sciences, St. Petersburg, Russian Federation; ORCID 0000-0001-5187-9615; e-mail: iraglebova@mail.ru

**Vadim I. Voshchikov**, Postgraduate, Research Engineer, Institute of Silicate Chemistry of Russian Academy of Sciences, St. Petersburg, Russian Federation; ORCID 0000-0001-9534-9157; e-mail: voshikoff@yandex.ru

**Шилова Ольга Алексеевна**, доктор химических наук, профессор, главный научный сотрудник, Институт химии силикатов им. И. В. Гребенщикова Российской академии наук, Санкт-Петербург, Российская Федерация; профессор базовой кафедры Санкт-Петербургского государственного электротехнического университета «ЛЭТИ», Санкт-Петербург, Российская Федерация; ORCID 0000-0002-3856-9054; e-mail: olgashilova@bk.ru

**Глебова Ирина Борисовна**, научный сотрудник, Институт химии силикатов им. И. В. Гребенщикова Российской академии наук, Санкт-Петербург, Российская Федерация; ORCID 0000-0001-5187-9615; e-mail: iraglebova@mail.ru

**Вошиков Вадим Иванович**, аспирант, инженер-исследователь, Институт химии силикатов им. И. В. Гребенщикова Российской академии наук, Санкт-Петербург, Российская Федерация; ORCID 0000-0001-9534-9157; e-mail: voshikoff@yandex.ru

**Valery L. Ugolkov**, Cand. Sc. (Eng.), Senior Researcher, Institute of Silicate Chemistry of Russian Academy of Sciences, St. Petersburg, Russian Federation; ORCID 0000-0003-2895-0625; e-mail: [ugolkov@isc.nw.ru](mailto:ugolkov@isc.nw.ru)

**Valerii Yu. Dolmatov**, D. Sc. (Eng.), Head of Research Laboratory, Special Design and Technology Bureau "Technolog", St. Petersburg, Russian Federation; ORCID 0000-0001-8643-0404; e-mail: [diamondcentre@mail.ru](mailto:diamondcentre@mail.ru)

**Ksenia A. Komarova**, Cand. Sc. (Veterinary), Research Scientist, A.N. Severtsov Institute of Ecology and Evolution of the Russian Academy of Science, Moscow, Russian Federation; ORCID 0000-0003-2378-6280; e-mail: [wtc-karpov@rambler.ru](mailto:wtc-karpov@rambler.ru)

**Aleksandra G. Ivanova**, Cand. Sc. (Chem.), Head of the Laboratory of Inorganic Synthesis, Institute of Silicate Chemistry of Russian Academy of Sciences, St. Petersburg, Russian Federation; ORCID 0000-0002-2129-7048; e-mail: [agp-13@inbox.ru](mailto:agp-13@inbox.ru)

**Уголков Валерий Леонидович**, кандидат технических наук, старший научный сотрудник, Институт химии силикатов им. И. В. Гребенщикова Российской академии наук, Санкт-Петербург, Российская Федерация; ORCID 0000-0003-2895-0625; e-mail: [ugolkov@isc.nw.ru](mailto:ugolkov@isc.nw.ru)

**Долматов Валерий Юрьевич**, доктор технических наук, начальник научно-исследовательской лаборатории, СКТБ «Технолог», Санкт-Петербург, Российская Федерация; ORCID 0000-0001-8643-0404; e-mail: [diamondcentre@mail.ru](mailto:diamondcentre@mail.ru)

**Комарова Ксения Александровна**, кандидат ветеринарных наук, научный сотрудник, Институт проблем экологии и эволюции им. А. Н. Северцова Российской академии наук, Москва, Российская Федерация; ORCID 0000-0003-2378-6280; e-mail: [wtc-karpov@rambler.ru](mailto:wtc-karpov@rambler.ru)

**Иванова Александра Геннадьевна**, кандидат химических наук, заведующая лабораторией неорганического синтеза, Институт химии силикатов им. И. В. Гребенщикова Российской академии наук, Санкт-Петербург, Российская Федерация; ORCID 0000-0002-2129-7048; e-mail: [agp-13@inbox.ru](mailto:agp-13@inbox.ru)

*Received 20 June 2022; Accepted 02 August 2022; Published 12 October 2022*



**Copyright:** © Shilova OA, Glebova IB, Voshchikov VI, Ugolkov VL, Dolmatov VYu, Komarova KA, Ivanova AG, 2022. This article is an open access article distributed under the terms and conditions of the Creative Commons Attribution (CC BY) license (<https://creativecommons.org/licenses/by/4.0/>).